COMITATO NAZIONALE PER L'ENERGIA NUCLEARE
Laboratori Nazionali di Frascati

LNF-75/6(R)
3 Febbraio 1975

A. Renieri: POSSIBILITY OF ACHIEVING VERY HIGH ENERGY RESOLUTION IN ELECTRON-POSITRON STORAGE RINGS.

Servizio Documentazione
dei Laboratori Nazionali di Frascati del CNEN
Casella Postale 70 - Frascati (Roma)

Laboratori Nazionali di Frascati del CNEN
Servizio Documentazione

LNF - 75/6
3 Febbraio 1975

A. Renieri: POSSIBILITY OF ACHIEVING VERY HIGH ENERGY RESOLUTION IN ELECTRON-POSITRON STORAGE RINGS. -

INTRODUCTION. -

The energy dispersion of the existing electron-positron storage rings is very large with respect to the energy width of the recent discovered narrow 3.1 and 3.7 GeV resonances[1 ÷ 4]. In Adone, for example, the full width half maximum center of mass energy dispersion is about 3 MeV (ref. 5 ÷ 8) (at 1.5 GeV), while the 3.1 GeV resonance width is of the order of 100 KeV.

The energy dispersion of electron-positron storage ring beams essentially depends on the radius of the bending magnets only[9] (for a given working energy). We have indeed,

$$(1) \qquad \sigma_p = \left(\frac{\Delta E}{E_o}\right)_{\text{r. m. s.}} \approx 4.35 \frac{\gamma}{\sqrt{\varrho}} \; 10^{-7}$$

Where we have put,

$\gamma = E_o/(m_o c^2)$ = ratio between the working energy and the electron rest energy.

ϱ = magnetic bending radius.

It can be seen from eq. (1) that the dependence of σ_p on ϱ is very weak. So that we cannot obtain a significant improvement of the energy resolution by merely increasing the magnetic radius ϱ.

Two alternative methods have been proposed[18, 19] to achieve a high center of mass energy resolution. They utilise the correlation existing between the transverse position and the displacement ΔE from the synchronous energy of a particle travelling inside a storage ring, as given by the off-energy function ψ[10]. In this paper we discuss the first one[18] at some length.

1. - THE METHOD. -

If the off-energy function ψ is equal for the two beams, an electron with a given energy, for example $E_o + \Delta E$, collides only with a positron having the same energy (neglecting the betatron motion[11]). The center of mass energy is then $2E_o + 2\Delta E$ (see Fig. 1).

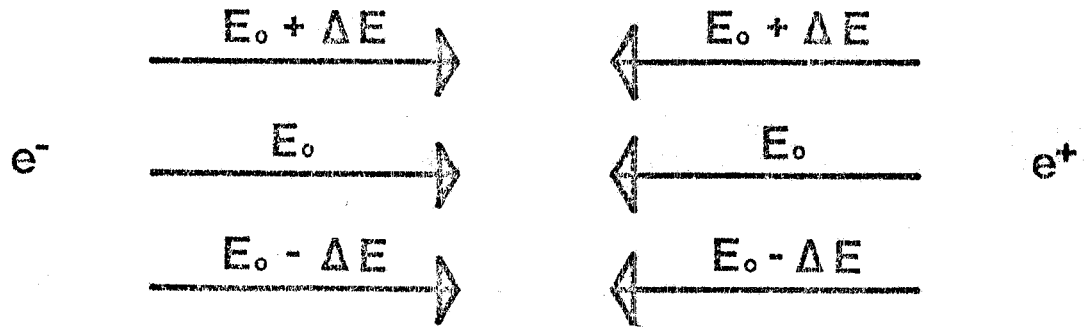

FIG. 1

But if the electron ψ function has the opposite sign with respect to the positron one, an electron with energy $E_o + \Delta E$ collides with a positron with energy $E_o - \Delta E$ (see Fig. 2).

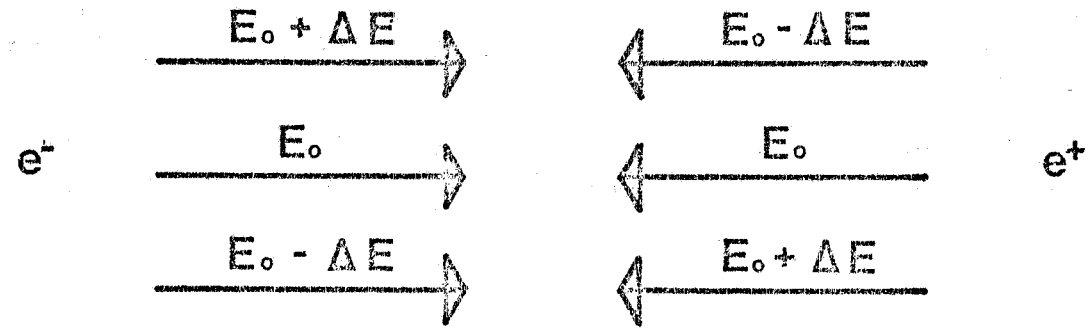

FIG. 2

Then we have, in the center of mass, the energy $2E_o$ for all collisions (we can neglect the center of mass motion energy, because it is of the order of $E_o(\Delta E/E_o)^2$). We must recall, however, that the betatron motion mixes the energies inside the beams. In the next section we compute the center of mass energy dispersion, taking into account both the transverse synchrotron and betatron motions.

2. - CENTER OF MASS ENERGY DISPERSION. -

We assume that in our storage ring the radial ψ is the same for e^+ and e^-, and the vertical one has opposite sign for the two beams.

We may generate opposite ψ_z's by using electrical bending elements (vertical electrodes).

We will use the following notations,

σ_x = r. m. s. radial betatron dimension
σ_z = r. m. s. vertical betatron dimension
ψ_x = radial off-energy function
ψ_z = vertical off-energy function
} at the crossing point

$\sigma_p = \Delta E/E_o$ = r. m. s. beam energy dispersion
E = particle energy, E_o = synchronous energy
E_B = center of mass energy
$p = (E-E_o)/E_o$, $p_B = (E_B-2E_o)/2E_o$.

The distribution function in x, z and p of the $e^{\pm}$ beam $g_{\pm}$ is given by,

$$(2) \qquad g_{\pm}(x,z,p) = \frac{N}{(2\pi)^{3/2}\,\sigma_x\,\sigma_z\,\sigma_p}\, e^{-\frac{(x-\psi_x\sigma_p)^2}{2\sigma_x^2}}\, e^{-\frac{(z\pm\psi_z\sigma_p)^2}{2\sigma_z^2}}\, e^{-\frac{p^2}{2\sigma_p^2}}$$

where N is the number of particles per bunch (we assume that all bunches are identical). The luminosity, as a function of p_B (the relative displacement of the center of mass energy from $2E_o$), is given by the following equation, (head-on collision)

$$(3) \qquad \frac{dL(p_B)}{dp_B} = 2\, f_o\, h \iiint_{-\infty}^{+\infty} dx\, dz\, dp\; g_+(x,z,2p_B-p)\; g_-(x,z,p)$$

where f_o is the particle revolution frequency in the ring and h is the number of bunches per beam. From eqs. (2) and (3) we obtain,

$$(4) \qquad \frac{dL(p_B)}{dp_B} = \frac{L_o}{\sqrt{2\pi}\;\sigma_T}\, e^{-\frac{p_B^2}{2\sigma_T^2}}$$

where we have put,

$$(5) \qquad \sigma_T = \frac{\sigma_p}{\sqrt{2}}\,\frac{1}{\sqrt{1+(\psi_z\sigma_p/\sigma_z)^2}}$$

$$(6) \qquad L_o = \frac{f_o\, h\, N^2}{4\pi\sqrt{(\sigma_x^2+\psi_x^2\sigma_p^2)(\sigma_z^2+\psi_z^2\sigma_p^2)}}$$

L_o is the luminosity integrated over all center of mass energies. If also ψ_x has opposite sign for the two beams, eqs. (5) and (6) become,

(7) $$\sigma_T = \frac{\sigma_p}{\sqrt{2}} \frac{1}{\sqrt{1 + (\frac{\psi_x \sigma_p}{\sigma_x})^2 + (\frac{\psi_z \sigma_p}{\sigma_z})^2}}$$

(8) $$L_o = \frac{f_o h N^2}{4\pi \sigma_x \sigma_z \sqrt{1 + (\frac{\psi_x \sigma_p}{\sigma_x})^2 + (\frac{\psi_z \sigma_p}{\sigma_z})^2}}$$

Let us consider now eq. (5). It can be seen that, in order to minimize σ_T, ψ_z must satisfy the condition,

(9) $$\psi_z \gg \frac{\sigma_z}{\sigma_p}$$

This means that the synchrotron vertical dimension must be very large with respect to the betatron one. Eq. (9) is equivalent to,

(10) $$\frac{\psi_z^2}{2 \beta_z} \gg \bar{H}_z$$

having used the equation

(11) $$\sigma_z = \sqrt{2 \bar{H}_z \beta_z} \; \sigma_p$$

In general $\bar{H}_z$ is given by two terms. The first one arises from the mean value of the invariant H_z[12] in the bending elements. The second one is due to the residual coupling between radial and vertical motion.

If the vertical off-energy function is identically null in the radial bending magnets (where the emission of synchrotron radiation is maximum, and therefore there is the maximum radiation noise), $\bar{H}_z$ is given essentially by the residual coupling ($H_z = \varepsilon^2$, H_x, ε = coupling factor).

In conclusion, in our machine we must satisfy the following conditions;

i : $\psi_z = 0$ in the radial bending magnets,
ii : low radial invariant $\bar{H}_z$ (in order to keep $\bar{H}_z = \varepsilon^2 \bar{H}_x$ low),
iii: working point as far off coupling as possible.

In order to satisfy condition i) we must design the experimental insertions (outside of which $\psi_z = 0$), without radial bending magnets.

Condition ii) requires a high ν_x per standard cell and high periodicity. Condition iii) implies that we must work with $\Delta\nu_x \neq \Delta\nu_z$ ($\Delta\nu_{x,z}$ is the non-integer part of $\nu_{x,z}$). Furthermore we must try to avoid causes lending to coupling the vertical motion to the radial one. Beam-beam interaction is of course just one of the unavoidable causes. Actually the two beams transverse cross section at the crossing point is shown in Fig. 3. We have this configuration because the off-energy function does not lie in a plane, and the vertical component is of opposite sign for the two beams. So that each beam appears to the other one as a skew quadrupole. The rotation angle θ is given by, (see App. A)

$$\theta = \frac{1}{2}\,\mathrm{arctg}\left(\frac{2\,\psi_x\,\psi_z\,\sigma_p^2}{(\sigma_x^2 + \psi_x^2\,\sigma_p^2) - (\sigma_z^2 + \psi_z^2\,\sigma_p^2)}\right) \tag{12}$$

In order to reduce θ, we have two possibilities (for fixed ψ_z, σ_z and σ_x), namely,

a) make ψ_x very large ($\theta \approx \frac{1}{2}\,\mathrm{arctg}\,(\frac{2\,\psi_z}{\psi_x}) \longrightarrow 0$),

or

b) $\psi_x = 0$.

The first choice is conditioned by the Amman longitudinal effect[13], which sets an upper limit to the quantity ψ_x^2/β_x at the crossing point. With the parameter of the proposed machine (high $\nu_x \longrightarrow$ low momentum compaction), the limit is very low (see App. B). We must therefore choose solution b) ($\psi_x = 0$). This condition limits the maximum luminosity per bunch that can be achieved, but (see sect. 5) not too strongly. In addition, with the choice b), there is complete overlap between the two beams. The non linear terms of the interaction are thus minimum.

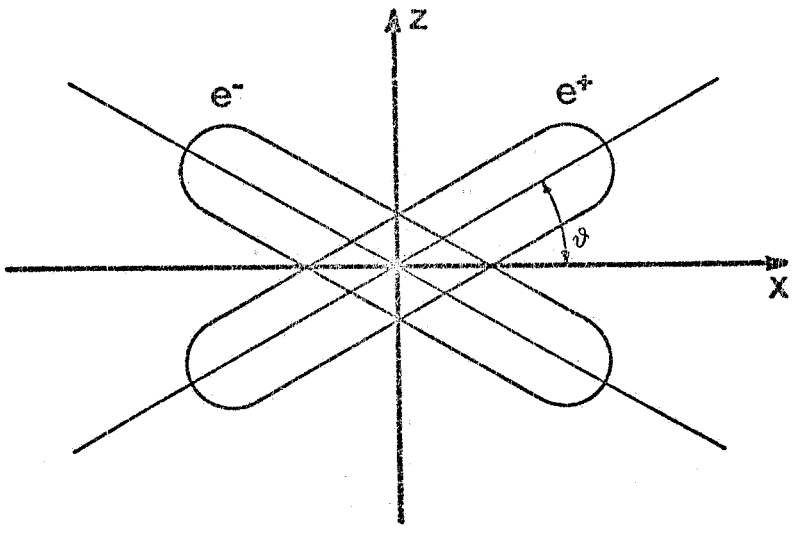

FIG. 3

This is a very important condition, because the transverse incoherent limit[14] seems to arise essentially from the non-linear terms of the interaction.

3. - THE MACHINE LATTICE. -

In this section we present, as an example, a machine with the magnetic bending radius $\varrho = 40$ m. This choice is a compromise between the requirement of a large radius, in order to minimize σ_p (see eq. (1)), and the possibility of operating the machine at the energies of $1.5 \div 2$ GeV per beam (where are the narrow resonances) with the bending magnetic field not too low. With this radius we may operate (in the conventional way, $\psi_z = 0, \psi_x \neq 0$), up to energies of the order of $7 \div 8$ GeV per beam. We remark that the proposed lattice is far from being fully optimized.

The machine layout is given in Fig. 4. The most important parameters are listed in Tab. I.

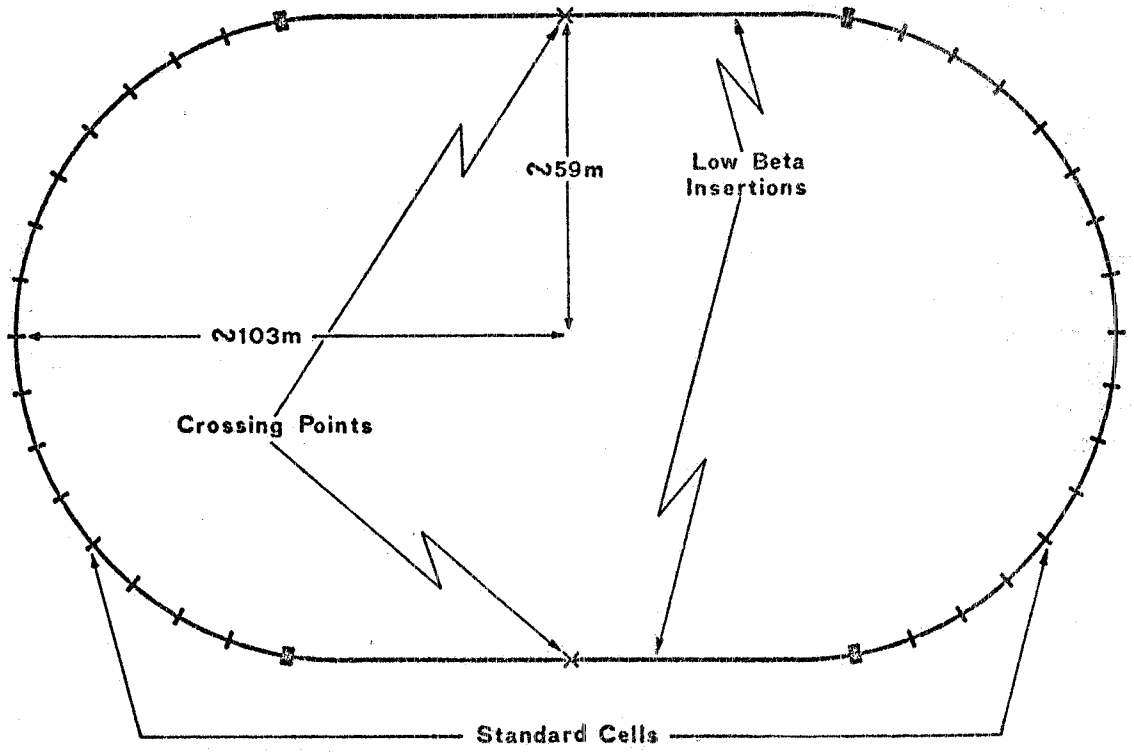

FIG. 4

Electrons and positrons travel in the same ring. They collide (head-on) in the center of the low-beta insertions. In the machine (see Fig. 4) there are 32 standard cells and two low-beta insertions. The standard cell layout and the corresponding optical functions β_x, β_z and ψ_x are given in Fig. 5.

In Fig. 6 we have the layout and the optical functions for the half insertion (the insertion is specular with respect to the crossing point).

TABLE I

(All energy dependent parameters are computed at E = 1.5 GeV)

Stored particles		e^+, e^-	
Beam energy	min	1.5	GeV
	max	8	GeV
Radiated energy per turn		13	KeV
Bending magnetic radius		40	m
Mean radius of the machine		86.5	m
Orbit length		543.5	m
Number of bending magnets		76	
Number of quadrupoles		114	
Number of standard cells		32	
Number of experimental low-beta sections		2	
Free low-beta straight section length per crossing		8	m
ν_x		16.20	
ν_z		13.15	
β_x		1.42	m
β_z		0.29	m
ψ_x		0.0	m
ψ_z		0.09	m
$\sigma_x^* = \sqrt{\sigma_x^2 + \psi_x^2 \sigma_p^2}$	at the crossing point	0.1	mm
$\sigma_z^* = \sqrt{\sigma_z^2 + \psi_z^2 \sigma_p^2}$	at the crossing point	0.02	mm
σ_x^*	maximum values	1.0	mm
σ_z^*	maximum values	0.1	mm
σ_p		2×10^{-4}	
$\overline{H}_x$		6.8×10^{-2}	m
α (momentum compaction)		7.1×10^{-3}	
τ_x	damping times	0.45	sec
τ_z	damping times	0.47	sec
τ_E	damping times	0.21	sec
$C_x = \frac{E_o}{\nu_x} \frac{d\nu_x}{dE}$	chromaticity	-3.71	
$C_z = \frac{E_o}{\nu_z} \frac{d\nu_z}{dE}$	chromaticity	-1.35	

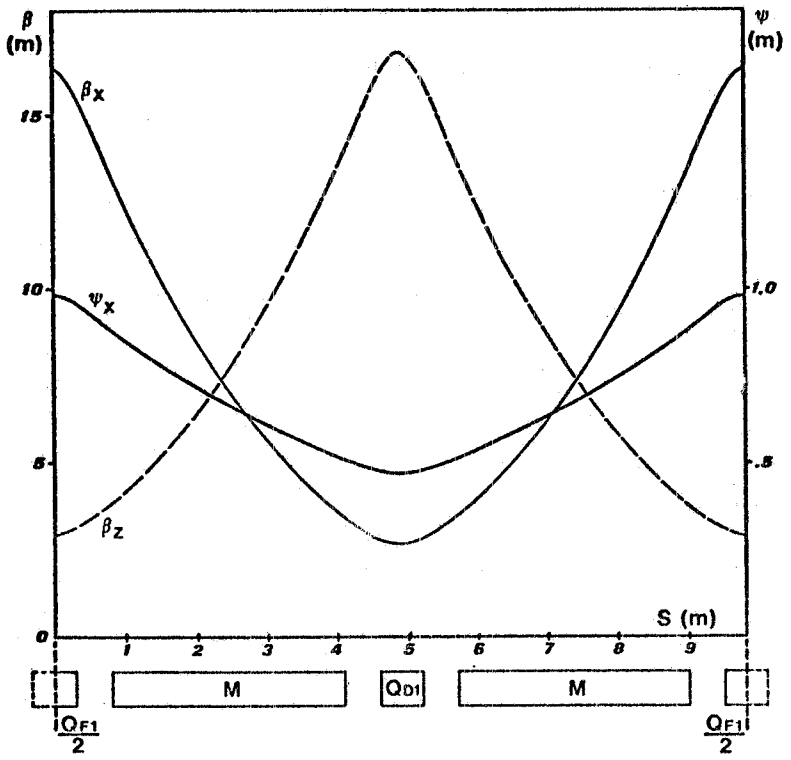

FIG. 5

The off-energy function ψ_z and the vertical orbit displacement from the machine simmetry plane Z in the insertion, are given in Fig. 7.

In Tabs.II and III we have the quadrupole and electrode characteristics respectively. The electric field quoted in Tab. III corresponds to a working energy E_o = 1. 5 GeV (near the narrow resonances). The field value requested (~10 KV/cm) is not too high. It is possible to have up to ~20 KV/cm over an electrode distance of about 10 cm, without excessive difficulties. Then we may operate with high center of mass energy resolution up to ~3 GeV per beam. We use the following notations,

Q_F = radial focusing quadrupole
Q_D = vertical focusing quadrupole
M = bending magnet
$K = \sqrt{G/B\varrho}$, G = quadrupole magnetic gradient
B, ϱ = magnetic field and radius of the bending magnets
E = vertical electrode
L_Q, L_E = quadrupole and electrode length.

The vertical displacement (~5 cm) in quadrupoles Q_{F4} and Q_{D5} (see Fig. 7) is high. So that their inner radius must be larger than that of the other quadrupoles. Furthermore their field quality must be very good, in order to avoid too high non linear spurious terms that may generate dangerous stop-bands.

TABLE II

Quadrupole	K (m)	L_Q (m)
Q_{F1}	0.721	0.6
Q_{D1}	0.707	0.6
Q_{D2}	0.724	0.6
Q_{F2}	0.792	0.6
Q_{D3}	0.616	1.0
Q_{F3}	0.774	1.0
Q_{D4}	0.648	0.6
Q_{F4}	0.635	2.0
Q_{D5}	0.647	2.0
Q_{D6}	0.733	1.0
Q_{F5}	0.707	1.0
Q_{F6}	0.582	1.0
Q_{D7}	0.756	1.0

TABLE III

Electrode	Electric field (KV/cm)	L_E (m)
E_1	9	5.5
E_2	-9	5.5
E_3	10	6.0

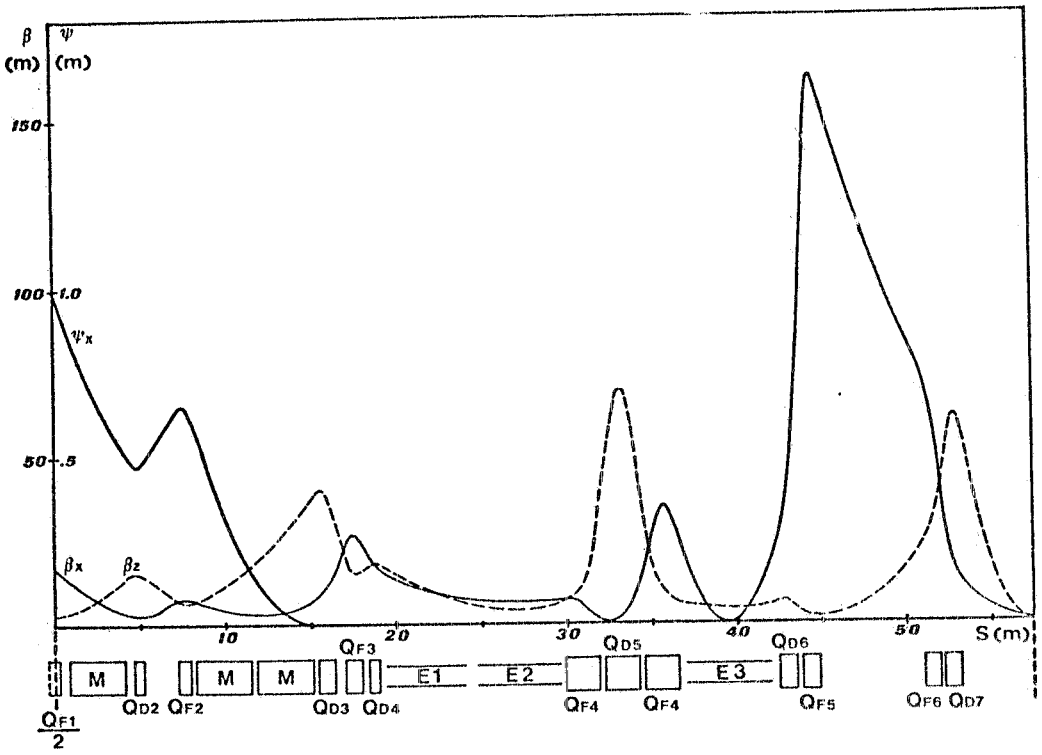
β (m)
ψ (m)
150
100
50
1.0
.5
ψx
βx
βz
10
20
30
40
50
S (m)
QF3
QD5
QD6
M
M
M
E1
E2
E3
QF1/2
QD2
QF2
QD3
QD4
QF4
QF4
QF5
QF6
QD7

FIG. 6

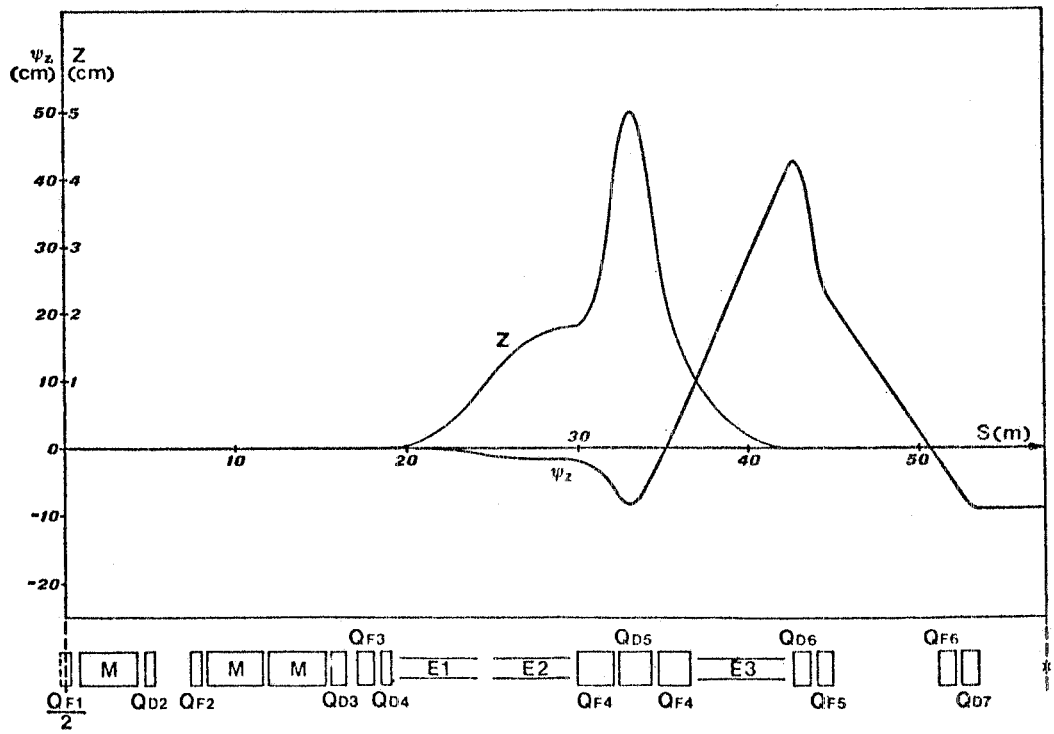
ψz (cm)
Z (cm)
50
40
30
20
10
0
-10
-20
5
4
3
2
1
Z
ψz
10
20
30
40
50
S(m)
QF3
QD5
QD6
QF6
M
M
M
E1
E2
E3
QF1/2
QD2
QF2
QD3
QD4
QF4
QF4
QF5
QD7

FIG. 7

For injection and the r.f. accelerating system, we may use the long insertion straight sections not used for experiments. The total free length is about 100 m.

From Table I we see that the natural machine chromaticity ($C_{x,z} = (E_o/\nu_{x,z})(d\nu_{x,z}/dE)$) is too high. It must be reduced by means of sextupoles, in order to avoid the head-tail instability[16] and to limit the ν spread across the beam. This is important especially during injection, when the energy dispersion may be very high. The sextupoles may be placed near the quadrupoles of the standard cells.

During the injection phase the beams must be kept separate[17]. For this purpose we can use electrodes E_1, E_2 and E_3 (see Fig. 7). If multibunch operation is envisaged (in order to increase the luminosity, see sect. 5), the beams must be kept separate also outside the insertion, and other electrodes (radial or vertical) must be arranged along the machine.

4. - CENTER OF MASS ENERGY DISPERSION. -

From eqs. (11) and (5) we obtain,

$$\sigma_T = \frac{\sigma_p}{\sqrt{2}} \frac{1}{\sqrt{1 + \frac{\psi_z^2}{2\,\beta_z \bar{H}_z}}} \tag{13}$$

$\bar{H}_z$ (see sect. 2) is due to the residual coupling between radial and vertical motion. We may assume,

$$\bar{H}_z \approx 10^{-2}\, \bar{H}_x \tag{14}$$

Under this assumption, the vertical betatron dimension is 1/10 of the radial one (for the same β). From eqs. (13) and (14) and using Table I, we obtain,

$$\sigma_T \approx 3 \times 10^{-5} \tag{15}$$

The center of mass absolute energy spread is,

$$\Delta E = 2E_o\, \sigma_T = 90 \text{ KeV} \quad (E_o = 1.5 \text{ GeV}) \tag{16}$$

that is, in terms of full width half maximum energy spread,

$$\Delta E_{FWHM} \cong 210 \text{ KeV} \tag{17}$$

For $E_o = 1.85$ GeV (corresponding to the 3.7 GeV resonance), we have, ($\Delta E \propto E_o^2$)

(18) $$\Delta E_{FWHM} = 300 \text{ KeV}$$

We remark that in a conventional machine a resolution such as that given by eq. (17) is only obtained with a very large magnetic bending radius ($\varrho \approx 1000$ m).

From eq. (17) we obtain,

(19) $$\frac{\Delta E_{FWHM}}{2E_o} \approx 7 \times 10^{-5} \quad (E_o = 1.5 \text{ GeV})$$

then we must require an energy stability of the machine much better than this value. If we have, (B = magnetic bending field)

(20) $$\left[\frac{\Delta B}{B}\right]_{\text{bending magnets}} \approx 10^{-5}$$

the center of mass energy fluctuation is negligible. We have indeed,

(21) $$\Delta E_B = 2E_o \left(\frac{\Delta B}{B}\right) \approx 30 \text{ KeV} \quad (E_o = 1.5 \text{ GeV})$$

5. - LUMINOSITY. -

The luminosity per bunch is relatively low. This is due to the small beam transverse dimensions at the crossing point. We have indeed:

i) high $\nu_x \rightarrow$ low $\overline{H}_x$,
ii) $\psi_x = o$ at the crossing point,
iii) operation off the coupling resonance.

The number of particles per bunch is then strongly limited by the beam-beam transverse incoherent effect[14], the values of β_x and β_z at the crossing point are as small as possible (for our insertion), and they are chosen in such a way that the radial limit is equal to the vertical one. The parameter used to express this limitation is the linear betatron tune shift due to the crossing (ΔQ). However, more frequently, the quantity ξ, that is proportional to the central beam density, is used. We assume that the maximum possible ξ is[14],

(22) $$\xi_{max} \approx 0.08$$

With this value, we obtain

(23) $$N = \text{number of particles per bunch} \approx 3 \times 10^9$$

From eqs. (6), (23) and from Table I we obtain, ($\beta_x \approx 1.4$ m, $\beta_z \approx 0.3$m)

$$\frac{L_o}{h} \approx 3.4 \times 10^{28} \text{ cm}^{-2} \text{ sec}^{-1} \quad (E_o = 1.5 \text{ GeV}) \tag{24}$$

If we want a luminosity of the order of magnitude of that of Adone, we must use a multibunch mode of operation. For example, with 8 bunches per beam we obtain

$$L_o \approx 3.10^{29} \text{ cm}^{-2} \text{ sec}^{-1} \tag{25}$$

We may obtain a further improvement of L_o by using a little more elaborate insertion, in order to have β_x and β_z smaller than 1.4 m and 0.3 m respectively. For example, with,

$$\beta_x \approx 35 \text{ cm}, \quad \beta_z \approx 7 \text{ cm} \tag{26}$$

we would get

$$\frac{L_o}{h} \approx 1.4 \times 10^{29} \text{ cm}^{-2} \text{ sec}^{-1} \tag{27}$$

so that, with 8 bunches, one has

$$L_o \approx 10^{30} \text{ cm}^{-2} \text{ sec}^{-1} \tag{28}$$

We must recall, however, that the counting rate on resonance is very high, even at relatively low luminosity. This is obviously due to the very high energy resolution of the machine. Finally we note that the value of ψ_z at the crossing point is well below that allowed by the longitudinal limit[13]. Actually the maximum admissible ψ_z is (see App. B).

$$(\psi_z)_{max} \approx .55 \text{ m} \tag{29}$$

to be compared (see Table I) with

$$\psi_z \approx 0.09 \text{ m} \tag{30}$$

6. - CONCLUDING REMARKS. -

We feel that it is possible to consider this low energy dispersion mode of operation as a facility that may be included, without difficulties, in any machine having special low-beta insertions, variable betatron tune and variable ψ_x at the crossing point, multibunch mode of operation and high stability of the guiding field (see eq. (20)). The only specific re-

quirement is the correct design of the large quadrupoles Q_{F4} and Q_{D5} (see sect. 3).

ACKNOWLEDGEMENTS. -

I am indebted to M. Bassetti, S. Tazzari, F. Tazzioli and G. Vignola for many useful discussions and suggestions.

REFERENCES. -

(1) - J. J. Aubert et al., Phys. Rev. Letters 33, 1404 (1974).
(2) - J. E. Augustin et al., Phys. Rev. Letters 33, 1406 (1974).
(3) - C. Bacci et al., Phys. Rev. Letters 33, 1408 (1974).
(4) - G. S. Abrams et al., Phys. Rev. Letters 33, 1453 (1974).
(5) - F. Amman, Frascati Report LNF-66/6 (1966).
(6) - M. Bassetti and S. Tazzari, Frascati Adone Internal Report E-14 (1974).
(7) - M. Bassetti, Frascati Adone Internal Report E-15 (1974).
(8) - M. Preger and A. Renieri, Frascati Adone Internal Report E-16 (1974).
(9) - M. Sands, The Physics of Electron Storage Rings, An Introduction, SLAC Report 121 (1970), pag. 124.
(10) - ibidem, pag. 70 (We use the notation ψ instead of η for the off-energy function).
(11) - ibidem, pag. 18.
(12) - ibidem, pag. 129.
(13) - F. Amman, Frascati Report LNF-71/82 (1971).
(14) - F. Amman, Proc. 1973 Particle Accelerator Conf., San Francisco (1973), pag. 858.
(15) - F. Amman et al., Frascati Report LNF-72/114 (1972), pag. 6.
(16) - C. Pellegrini, Nuovo Cimento 64A, 447 (1969).
(17) - A. Renieri, Frascati Adone Internal Report SM-15 (1973).
(18) - A. Renieri, Frascati Adone Internal Report E-17 (1974).
(19) - M. Bassetti, Frascati Adone Internal Report E-18 (1974).

APPENDIX A. -

From eq. (2) we obtain,

$$\int_{-\infty}^{+\infty} g(x,z,p)\,dp = \frac{N}{2\pi\sigma_x\sigma_z\sqrt{1+(\frac{\psi_x\sigma_p}{\sigma_x})^2+(\frac{\psi_z\sigma_p}{\sigma_z})^2}}$$

$$\text{(A1)}\qquad \exp\left\{-\frac{1}{2(1+(\frac{\psi_x\sigma_p}{\sigma_x})^2+(\frac{\psi_z\sigma_p}{\sigma_z})^2)}\left(\frac{x^2}{\sigma_x^2}(1+(\frac{\psi_z\sigma_p}{\sigma_z})^2)+\frac{z^2}{\sigma_z^2}(1+(\frac{\psi_x\sigma_p}{\sigma_x})^2-\right.\right.$$

$$\left.\left.-\frac{2xz\,\psi_x\psi_z\sigma_p^2}{\sigma_x^2\sigma_z^2}\right)\right\}$$

Eq. (A1) gives a transverse distribution function at the crossing point with the simmetry axis forming an angle θ with the (x, z) coordinate axis, θ is given by,

$$\text{(A2)}\qquad \theta = \frac{1}{2}\,\text{arctg}\left(\frac{2\psi_x\psi_z\sigma_p^2}{(\sigma_x^2+\psi_x^2\sigma_p^2)-(\sigma_z^2+\psi_z^2\sigma_p^2)}\right)$$

APPENDIX B. -

The Amman longitudinal effect[13] gives a limitation to the value of ψ^2/β that may be obtained at the crossing point. If we have radial and vertical ψ the limit may be written as follows

$$\text{(B1)}\qquad \frac{4m}{R}\left(\xi_x\frac{\psi_x^2}{\beta_x}+\xi_z\frac{\psi_z}{\beta_z}\right) < \alpha \quad \text{at the crossing point}$$

where α is the unperturbed momentum compaction, m is the number of crossing points, R is the machine mean radius, ξ_x and ξ_z are defined in sec. 5. From Table I we obtain,

$$\psi_x = 0, \qquad m = 2, \qquad R = 86.5\ \text{m}, \qquad \alpha = 7.1\times10^{-3}$$

from eq. (22) we have $\xi_x \approx \xi_z \approx 0.08$, so that

$$\text{(B2)}\qquad \frac{\psi_z^2}{\beta_z} \lesssim 1\ \text{m}$$

with $\beta_z \approx 0.3$ m the maximum ψ_z is

(B3) $$(\psi_z)_{max} \approx 0.55 \text{ m}$$

From Table I we obtain

(B4) $$\frac{\psi_x^2}{\beta_z} \approx 3\times10^{-2} \ll 1 \text{ m}$$

the longitudinal limit is well satisfied. From eq. (B1) we may derive the maximum value for ψ_x^2/β_x. We obtain

(B5) $$\frac{\psi_x^2}{\beta_x} \lesssim 0.9 \text{ m}$$

For $\beta_x \approx 1.4$ m we have

(B6) $$\psi_x \lesssim 1 \text{ m}$$

From eq. (12) and Table 1 we obtain for ψ_x = 1m,

(B7) $$\theta \approx 0.07 \text{ rad} \approx 4^o$$

This value is too high. It may give a very strong coupling between radial and vertical motion.